

# We are IntechOpen, the world's leading publisher of Open Access books Built by scientists, for scientists

6,900

Open access books available

186,000

International authors and editors

200M

Downloads

Our authors are among the

154

Countries delivered to

TOP 1%

most cited scientists

12.2%

Contributors from top 500 universities



WEB OF SCIENCE™

Selection of our books indexed in the Book Citation Index  
in Web of Science™ Core Collection (BKCI)

Interested in publishing with us?  
Contact [book.department@intechopen.com](mailto:book.department@intechopen.com)

Numbers displayed above are based on latest data collected.  
For more information visit [www.intechopen.com](http://www.intechopen.com)



# Design and Development of Ultrasonic Process Tomography

Mohd Hafiz Fazalul Rahiman<sup>1</sup>, Ruzairi Abdul Rahim<sup>2</sup>,  
Herlina Abdul Rahim<sup>2</sup> and Nor Muzakkir Nor Ayob<sup>2</sup>

<sup>1</sup>*Universiti Malaysia Perlis (UniMAP)*

<sup>2</sup>*Universiti Teknologi Malaysia (UTM)*

<sup>1,2</sup>*Malaysia*

## 1. Introduction

Process tomography is a process of obtaining the plane-section images of a three-dimensional object. Process tomography techniques produce cross-section images of the distribution of flow components in a pipeline, and it offers great potential for the development, and verification of flow models, and also for process diagnostic.

The measurement of two-component flow such as liquid or oil flow through a pipe is increasingly important in a wide range of applications, for example, pipeline control in oil exploitation, and chemical process monitoring. Knowledge of the flow component distribution is required for the determination of flow parameters such as the void fraction, and the flow regime.

Real-time reconstruction of the flow image is needed in order to estimate the flow regime when it is continuously evolving. This flow image is important in many areas of industry, and scientific research concerning liquid/gas two-phase flow. The operation efficiency of such a process is closely related to accurate measurement, and control of hydrodynamic parameters such as flow regime, and flow rate (Rahiman et al., 2010). Commonly, the monitoring in the process industry is limited to either visual inspection or a single-point product sampling assuming the product is uniformed. This approach for the determination of fluid flow parameters of two-component flow is also known as flow imaging.

### 1.1 Principle overview

Ultrasonic sensors have been successfully applied in flow measurement, non-destructive testing, and it is widely used in medical imaging. The method involves in using ultrasonic is through transmitting, and receiving sensors that are axially spaced along the flow stream. The sensors do not obstruct the flow. As the suspended solids' concentration fluctuates, the ultrasonic beam is scattered, and the received signal fluctuates in a random manner about a mean value. This type of sensor can be used for measuring the flow velocity. Two pairs of sensors are required in order to obtain the velocity using a cross-correlation method. Ultrasonic sensor propagates acoustic waves within the range of 18 kHz to 20 MHz.

Ultrasonic wave is strongly reflected at the interface between one substance, and another. However, it is difficult to collimate, and problems occur due to reflections within enclosed spaces, such as metal pipes. There are two types of ultrasonic signals that are usually used. They are the continuous signal, and the pulsed signal. Using a continuous signal will provide continuous impact on the crystal whereas by using pulses the interval of the transmission and reception signal can be estimated. Using the ultrasonic method in the air is very inefficient due to the mismatch of the sensors' impedance as compared with air's acoustic impedance. New types of sensors are continually being developed, but the effective ones are expensive. The design of this sensor is critical when it needs to reduce the sensor's ringing.

### 1.2 The tomography technique

The first step of a tomographic process is to generate the integral measurements using a selected sensor. The second step is to reconstruct the property field (the cross-sectional distribution of the physical properties of the multiphase media) from the measured integral values. This process is called tomographic reconstruction (Warsito et al., 1999).

There are numerous reconstruction algorithms available for tomographic reconstruction. The algorithms based on Fourier's techniques, and the algebraic reconstruction technique (ART) has been widely used in the field of medicine. However, the choice of the reconstruction algorithm is also dependent on the sensor system selected. In engineering related applications, the number of measurement is usually very small to perform a real-time measurement or limited by constraints on the sensor employed. Therefore, the reconstruction results are then further corrected using a mathematical approximation to obtain a better reconstruction.

In contrast to light or other electromagnetic waves, ultrasound needs medium to transmit through, and interrogates the physical properties (i.e. density, compressibility) of the media. Therefore, it is speculated that such a method would be appropriate for application in a medium with relatively homogeneous but high density, which is poorly penetrated by light or other electromagnetic radiation. In addition, in comparison with high-energy electromagnetic radiation, ultrasonic technique consumes much lower energy, low-cost, and simpler to use, and suitable for applications from laboratory scale to industrial plants (Williams & Beck, 1995).

## 2. Ultrasonic process tomography – An overview

Instrumentation systems employing a variety of ultrasonic techniques have been applied to a wide range of measurements in the chemical, and process industries (Asher, 1983). At least, eight categories of ultrasonic flow meter can be identified with flow meters of time-of-flight type now being employed in single-phase liquid, and gas flow measurement with a great deal of success. It is favoured by most industries due to the benefits as follows (Asher, 1983):

- i. Ultrasonic techniques can usually be truly non-invasive.
- ii. It has 'no moving parts'.
- iii. The radioactive materials are not involved.
- iv. The rapid response usually in a fraction of a second.
- v. The energy levels required to excite the transducers are very low, and have no detrimental effect on the plant or the materials being interrogated.

- vi. A mutually compatible range of techniques can be used to determine a wide range of parameters: these include liquid level, interface position, concentration (or density), temperature, and flow-rate. Hence multiplexed electronics are feasible.

Besides, those benefits have a significant impact, and lead to the development of Ultrasonic tomography. Ultrasonic tomography offers the advantage of imaging two-component flows, and gives the opportunity of providing quantitative and real-time data on chemical media within a full-scale industrial process, such as filtration, without the need of process interruption (Warsito et al., 1999).

The major potential benefits are; it is possible to gain an insight into the actual process; secondly, since ultrasonic tomography is capable of on-line monitoring, it has the opportunity to develop closed-loop control systems, and finally, it can be a non-invasive, and possibly non-intrusive system. The overall anticipated effects are improvements in product yield, and uniformity, minimized input process material, reduced energy consumption, and environmental impact, and the lowering of occupational exposure to plant personnel.

The popular ultrasonic sensing system is the transmission-mode, and the reflection-mode. The transmission-mode technique is based on the measurement of the change in the properties of the transmitted acoustic wave, which are influenced by the material of the medium in the measuring volume. The change of the physical properties can be the intensity, and/or transmission time (time-of-flight). The reflection-mode technique is based on the measurement of the position, and the change of the physical properties of wave or a particle reflected on an interface. Similar to the reflection-mode technique there are some techniques based on diffraction or refraction of wave at a discrete or continuous interface in the object space.

Utilizing attenuation or time-of-flight of a transmitted energy beam such as light or acoustic waves to produce an image of multiphase flow has been attempted at an early stage. In transparent media, optical methods based on light transmission technique, and the photographic techniques has proven quite effective (Rahim et al., 2011). However, since many real reaction systems are optically opaque, an application of the elegant optical method is severely limited.

Techniques based on reflection or the scattering of optical or acoustical waves were realized by measuring the Doppler shift-frequency of the reflected or scattered signals. An example is the use of laser Doppler anemometry for in-situ measurements of velocity, fluctuating velocity, size, and concentration of particles, bubbles or droplets in multiphase systems. A corresponding example of the Doppler technique utilizing ultrasonic wave is the measurements of bubble velocity in a stirred tank, and a fermenter or vessel by Broring et al., (1991).

A combination of the transmission and the reflection modes is found in acoustical imaging techniques, which are widely used in medical, and ocean engineering fields from early stages. An application of ultrasonic imaging velocimetry has been attempted by Kytomaa & Corrington (1994) to investigate a transient liquefaction phenomenon of cohesion-less particulate media. More advanced particle imaging velocimetry techniques were developed by combining the photographic technique and image processing technique or using radioactive particle tracking techniques. Examples are using particle image velocimetry

(PIV), particle streak velocimetry (PSV), and particle tracking velocimetry (PTV) for visualizing the flow pattern of multiphase flows (Rashidi, 1997).

### 2.1 The attenuation model

The attenuation process may be modelled by Lambert's exponential law of absorption, where the ultrasonic energy intensity of transmitter and receiver are related as in Figure 1 and Equation (1), where  $L$  represents the total path length.

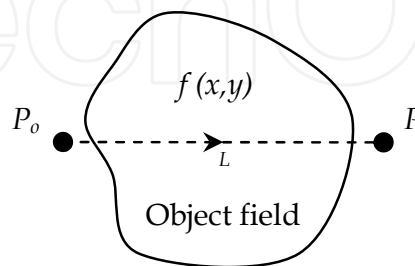


Fig. 1. The ultrasonic attenuation model

$$P = P_o \exp \left( - \int_L f(x,y) dP \right) \quad (1)$$

where  $P$  = the measured sound pressure (dB),  $P_o$  = the initial sound pressure (dB),  $L$  = path length in the object field (m), and  $f(x,y)$  = the attenuation function of the object field (dB/m). Because the pressure is proportional to the voltage measured by the transducer, Equation (1) can be written as Equation (2).

$$v_{Rx} = v_{Tx} e^{-\alpha L} \quad (2)$$

where  $v_{Rx}$  = the ultrasonic receiver voltage (V),  $v_{Tx}$  = the ultrasonic transmitted voltage (V), and  $\alpha$  = the attenuation coefficient of the object field (Np/m).

As introduced above, the attenuation will critically depend upon the material through which the ultrasonic wave travels.

### 2.2 Scattering issues

Acoustic impedance is a ratio of acoustic pressure to acoustic volume flow, and is frequency dependent. The greater the difference in acoustic impedance at the interface, the greater will be the amount of energy reflected. At a water, and gas interface, about 99.94% of the ultrasonic energy will be reflected (Rahiman et al., 2008). However, in some cases, scattering occurs on small gas hold-ups. Small was defined as a sphere with a radius of  $a$  where the circumference of the sphere,  $2\pi a$ , divided by the wavelength  $\lambda$  is much less than 1 (i.e.  $ka = 2\pi a/\lambda \ll 1$ ) where  $k$  is the wave number =  $2\pi f/c$ .

If ultrasonic waves propagate in a bubbly air/water with a wavelength much shorter than the gas radius  $a$ , i.e.  $ka \gg 1$ , the diffraction can be ignored, and these hold-ups will act as many acoustics opacities. This is because when  $ka \gg 1$ , the surface of the sphere appears as a flat surface with respect to the wavelength, and the scattering becomes the same as a reflection from a flat surface.

The relationship of the simplified ultrasonic transmission model is depicted in Equation (3), and shown graphically in Figure 2.

$$V_G = V_C - V_R \quad (3)$$

where  $V_G$  is the sensor loss voltage due to the gas opacity,  $V_C$  is the calibration voltage, and  $V_R$  is the receiving voltage. For measuring the concentration profile, the parameter  $V_G$  is to be resolved.

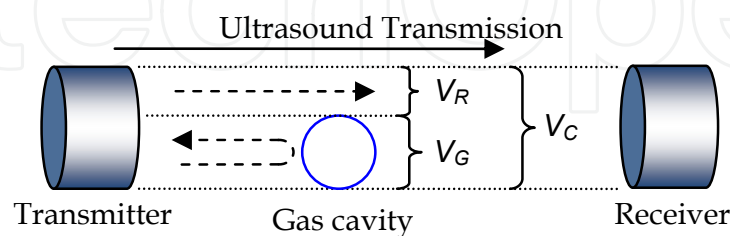


Fig. 2. The simplified ultrasonic transmission model

### 3. The measurement system

One of the most important parts in an ultrasonic tomography system is the front-end, which is the transducer array, and associated electronic hardware. This is important for acquiring the data needed to produce a meaningful image. This is fundamental to the success or failure of an acoustic imaging system. Therefore, given the object to be imaged, and the specifications to be achieved, the design of the front-end of an acoustic imaging system should be regarded as a first priority.

Ultrasonic transducer is a device capable of converting electrical energy into high-frequency sound waves, and also converting sound waves back into electrical energy. Ultrasonic transducer contains piezoelectric crystal materials that have the ability to transform mechanical energy into electrical energy, and vice versa. In reality, when a crystal element is pulsed with a voltage profile, a wave starts travelling from each face of the crystal element. The vibrational mode of the crystal can therefore, only be considered from a transient wave propagation viewpoint. Resolution and penetrating power of an ultrasonic wave depends on the resulting wavelength of excitation inside the material in question. Greater wavelengths or lower frequencies generally penetrate much further into a material (Kannath & Dewhurst, 2004). Higher frequency ultrasonic excitations with smaller wavelengths generally decay more rapidly inside a material, but resolution capability is improved.

For the presented systems, the active element for the transducers is the wide-angle beam ceramic piezoelectric with resonance frequency of 333 kHz. Transducer elements employed in ultrasonic imaging arrays may be designed to produce either a narrow focused beam or a divergent beam. The beam pattern used for two-dimensional imaging is the cylindrically diverging or 'fan-shaped' beam pattern. This is to ensure a maximum number of transducers located around the pipe circumference, which receive the directly transmitted wave.

### 3.1 Fan-shaped beam sensor array

An example of a fan-shaped beam sensor array is shown in Figure 3, which consists of 32-ultrasonic transceivers that is mounted on an experimental column. The transceivers enable the transmission, and reception on the same sensor. The transmission and reception of ultrasonic waves are, however, controlled by the electronic analogue-switches which direct the signal to the corresponding channels.

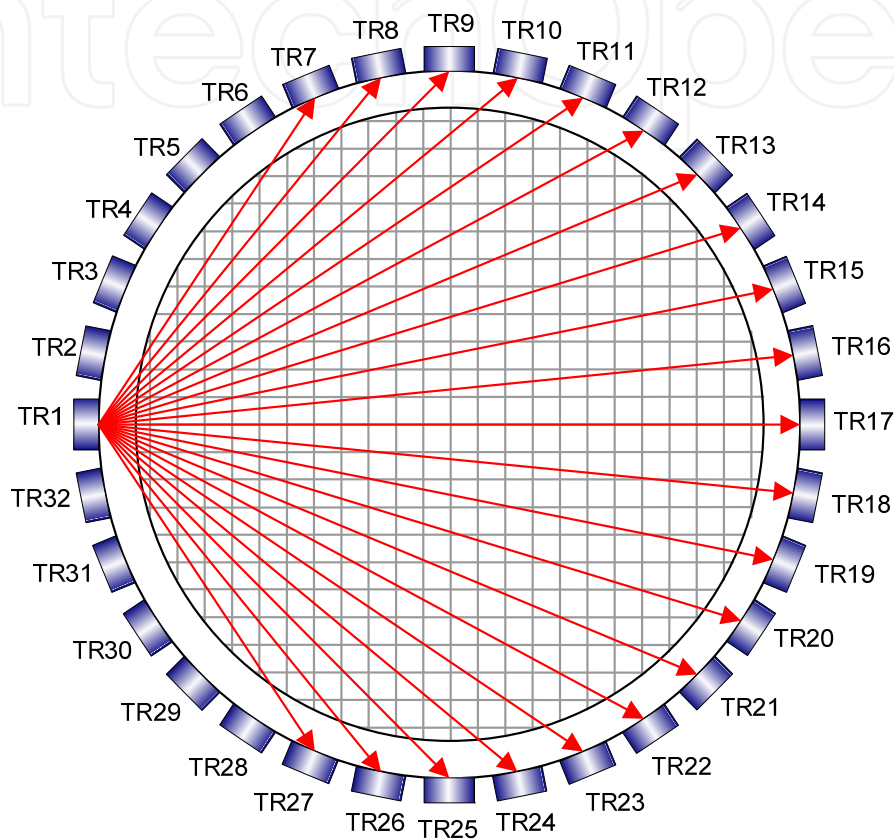


Fig. 3. Ultrasonic transceiver sensor array

One of the significant advantages in employing ultrasonic techniques is it enables measurement to be made without breaking into the process vessel, and therefore, measurements can be made where for a reason of safety hygiene, continuity of supply or cost it is not possible to break into the process vessel. However, the invasive transducers actually contact the flow inside the pipe, for obvious reasons it is not favoured by most industries (Sanderson & Yeung, 2002).

In Figure 3, the transmitter is modelled as a point source, which propagates within angle  $a$  in the image plane, and the receiver is modelled as a circular arc with radius of curvature  $r$ . The wavefronts are taken to be circular arcs of uniform ultrasonic energy. When ultrasound is propagating in the flow medium, areas occupied by the discontinuous component block the transmitted ultrasound. As a result, an effect analogous to the shadowing of visible light by an opaque object can be seen in Figure 4. An example of transmitting, and receiving ultrasonic signals is shown in Figure 5.

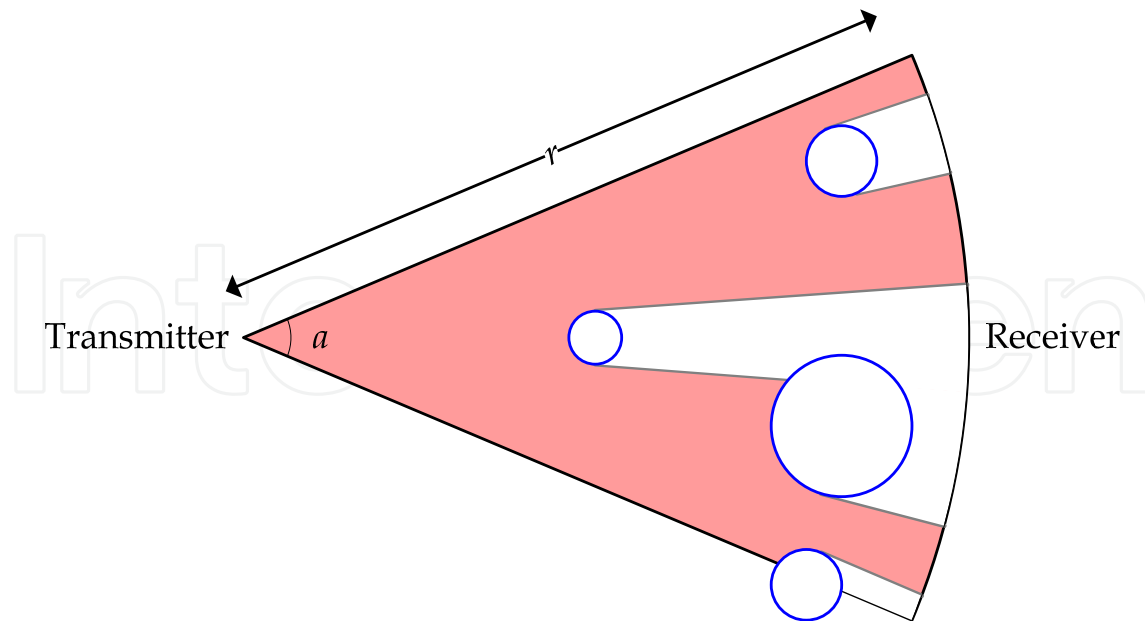


Fig. 4. The discontinuous component viewed by the ultrasonic receiver

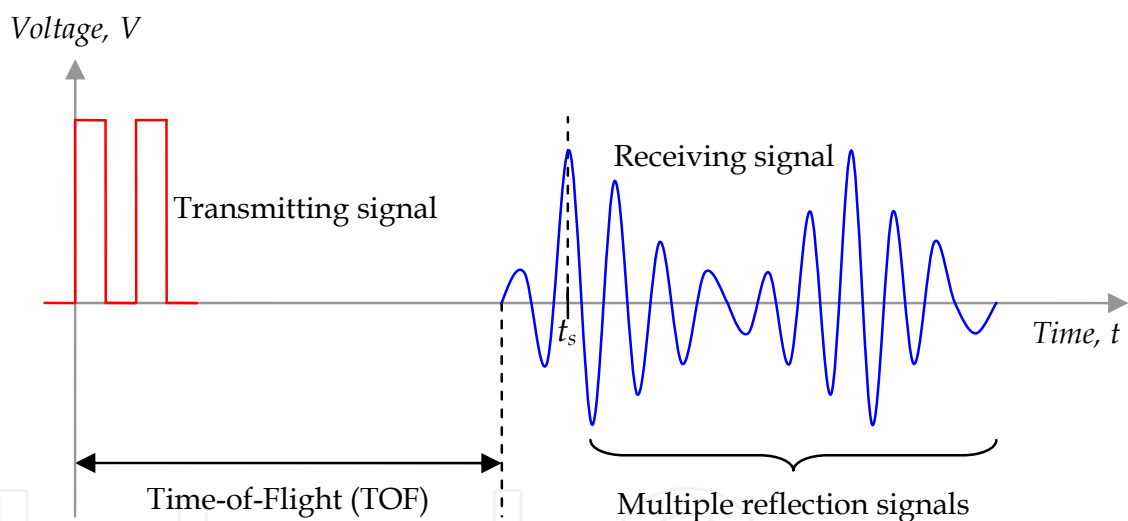


Fig. 5. An example of transmitting, and receiving an ultrasonic signal

In our work, a transmission-mode method emphasizing the receiver amplitude, and the arrival time analysis has been used. Arrival time analysis is based on the simple fact that it takes some finite time for an ultrasonic disturbance to move from one position to another inside the experimental pipe. In Figure 5, the *observation time* denoted by  $t_s$  was the first peak after the time-of-flight corresponding to a straight path. By sampling amplitude of this observation time for every receiving sensor due to projection of transmitters, the information via transmission-mode method can be obtained. As the distance between the transmitting sensor, and the receiving sensor increases, the ultrasound will consume longer time-of flight to reach to the point of interest, and therefore, set out a longer observation time. This time-of-flight may then be assumed to be proportional to the distance that they had travelled (Moore *et al.* 2000).

### 3.2 The system block diagram

The system block diagram is shown in Figure 6. The microcontroller will generate a burst tone of a two-cycle ultrasonic pulses at 333kHz with duty-cycle of 50% at each cycle. The delay between each burst tone was 6.667ms which is for the reverberation effect delays of the receiver before the next transmitting transceiver excited. An illustration of the pulses is shown in Figure 7. The reverberation effect delays are needed to avoid overlapping echoes at the receiving transceiver due to two separate ultrasound excitation. To select the corresponding transmitting, and receiving transceivers, several analogue switches have been utilized.

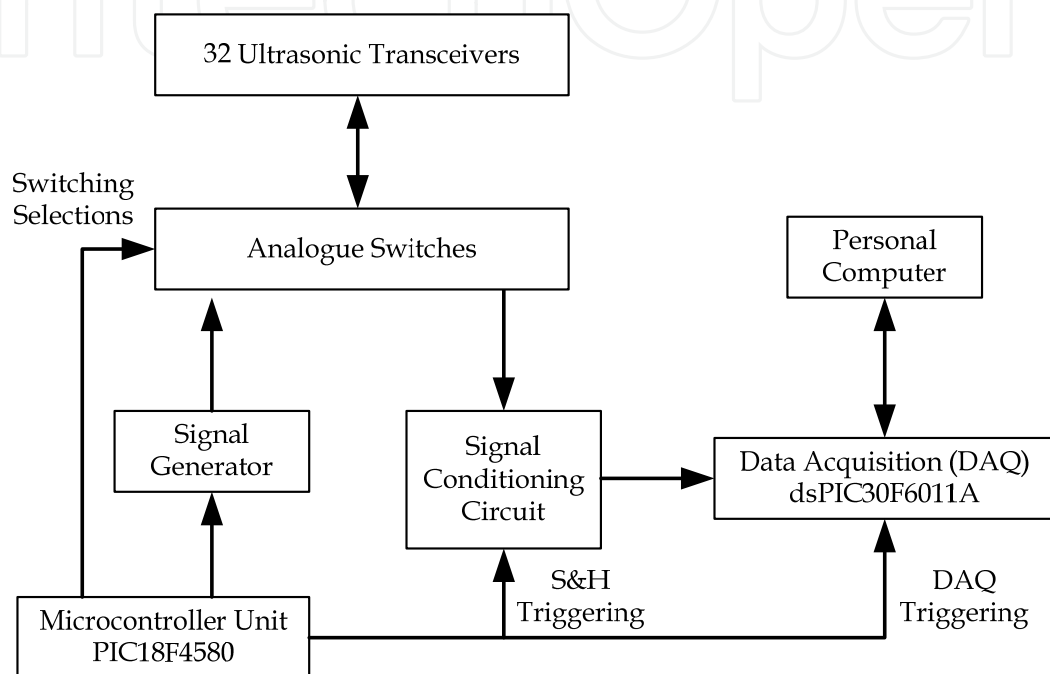


Fig. 6. The ultrasonic system block diagram

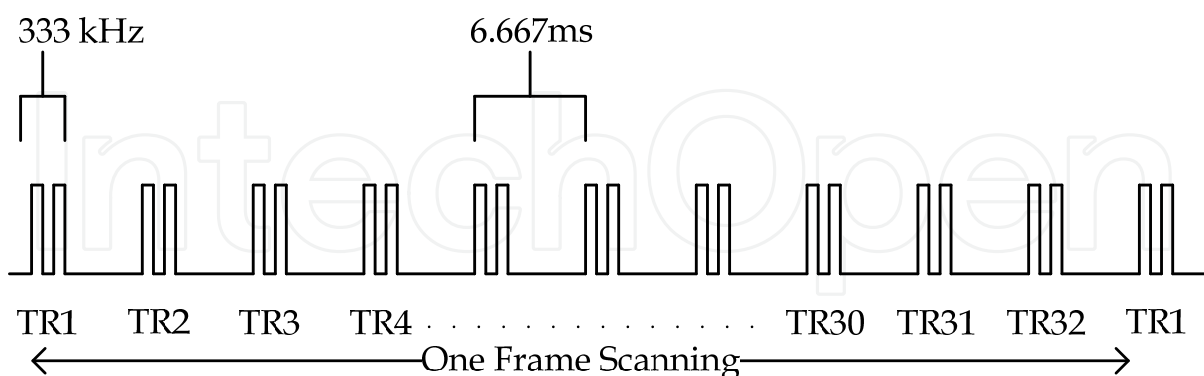


Fig. 7. The burst tones generated by microcontroller

The signal generator was designed using a low-noise high-speed op-amp, TLE2141 that acts as comparator. The comparator will generate a 20Vp-p burst tone of 333 kHz. The burst tone excitation is designed so that it is long enough for transient effects but short enough for the burst to be received without multiple reflections as describe previously. The circuit is shown in Figure 8.

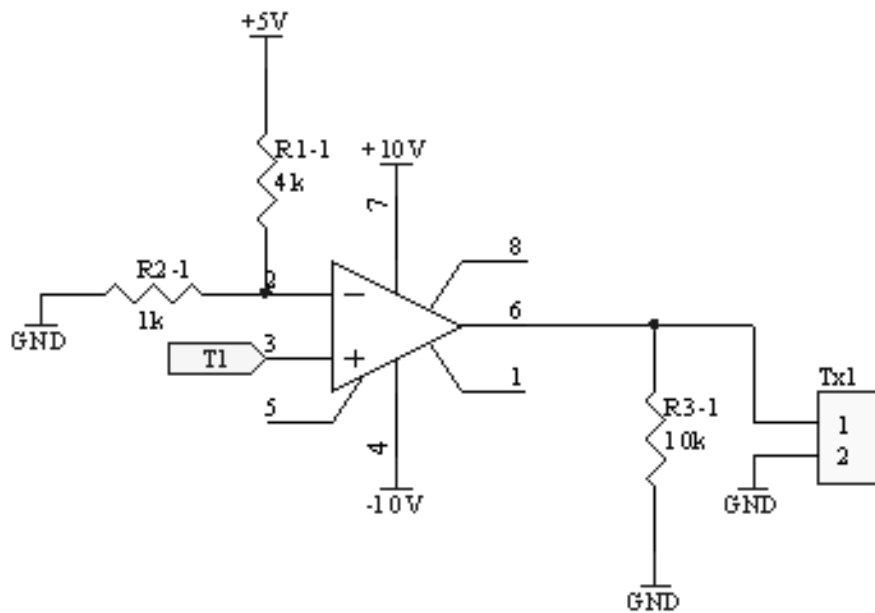


Fig. 8. The signal generator circuit

The signal conditioning circuit consists of two components where the first component is the amplifier, and the second component is the signal processing circuit that is the sample and hold circuit. The amplifier was built using a dual-wide gain bandwidth op-amp to avoid signal distortion during amplification. The amplifier uses two stages inverting op-amp design. Both the first stage and the second stage amplifier gain were set with -150. The signal conditioning circuit is shown in Figure 9.

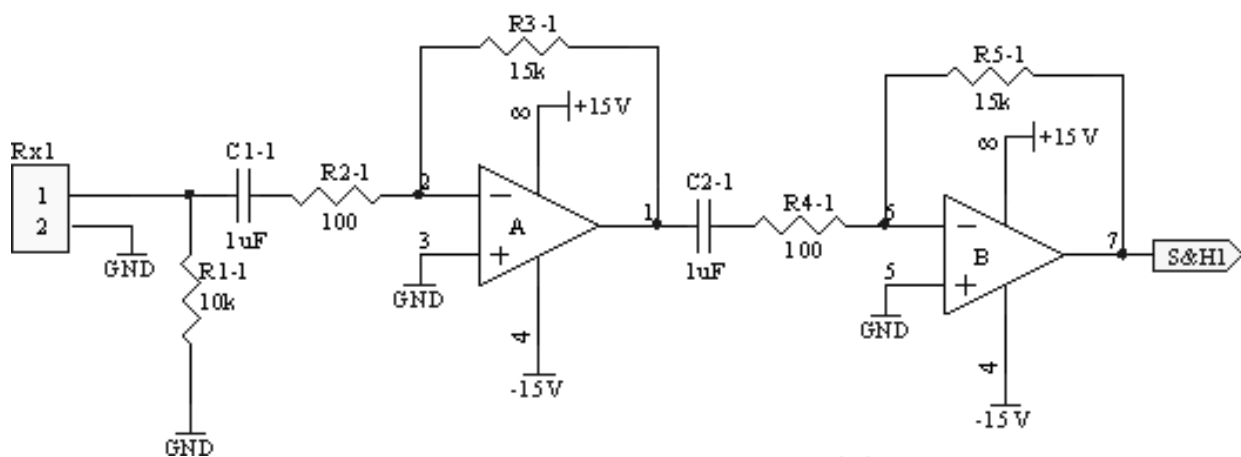


Fig. 9. The signal conditioning circuit

When the components to be imaged are gases, there may be no directly transmitted signals from the transmitter to the receiver because of the obstacles. By reflecting at the gas component surfaces, the receiver may still detect some signals but at a later time though because direct transmission takes the shortest path, and hence the shortest time. Thus, if the *observation time* is monitored, it is possible to test whether there are any objects between the transmitter, and the receiver. By sampling the signals at this observation time for every receiving transceiver, the spatial information in the measurement area can be obtained. To discriminate the exact information (information by the observation time) the sample and

hold method is used. A sample and hold circuit, also called a track-and-hold circuit is a circuit that captures, and holds an analogue voltage in a specific point in time under control of an external circuit (microcontroller). The operation of sample and hold is shown in Figure 10, and the circuit diagram for sample and hold is shown in Figure 11.

The holding signal is also known as the *sensor value* voltage will be sampled by the DAQ using the dsPIC30F6011A IC which served as the analogue-to-digital converter as well. The information captured by the DAQ will be processed, and send to the PC for generating the corresponding tomography images.

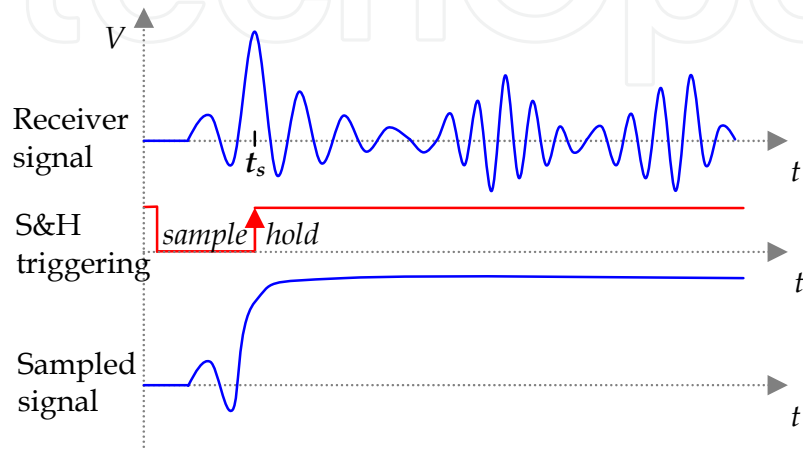


Fig. 10. The sample and hold operation

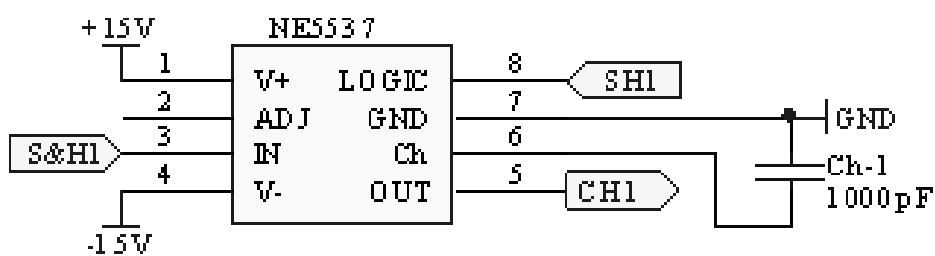


Fig. 11. The sample and hold circuit

## 4. Image reconstruction

In this work, the tomographic images are derived by using a back projection algorithm. In order to derive this algorithm, which results in the solution to the inverse problem, the forward problem must be solved first.

### 4.1 The forward problem

The forward problem determines the theoretical output of each of the sensors when the sensing area is considered to be two-dimensional. The cross-section of the pipe is mapped onto a  $64 \times 64$  rectangular array consisting of 4096 pixels. The forward problem can be solved by using the analytical solution of sensitivity maps, which produces the sensitivity matrices. Each transmitting sensor is virtually excited, and the affected pixels are taken into account (as shown in Figure 12).

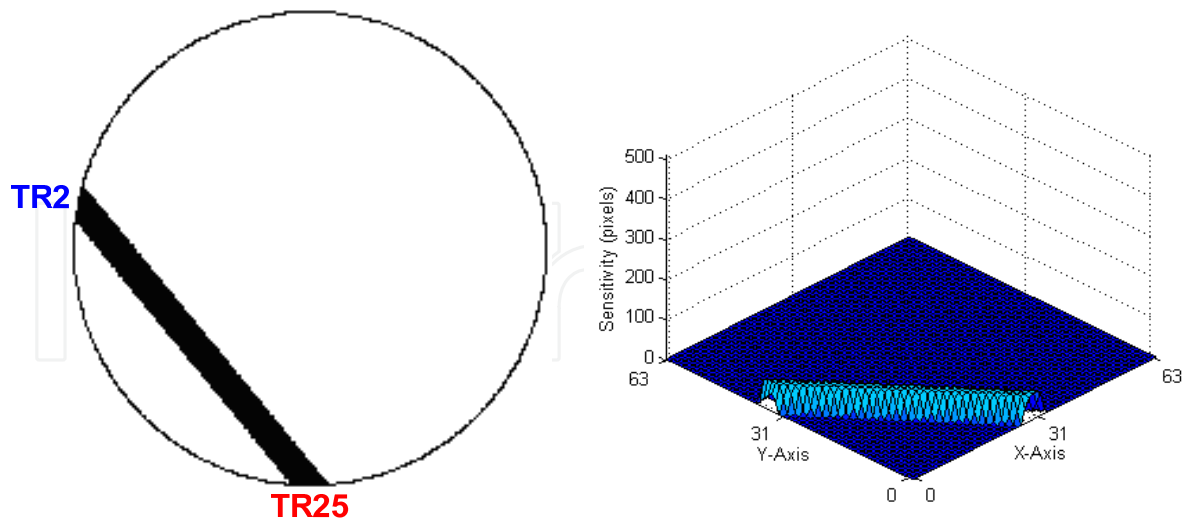


Fig. 12. The sensitivity map for projection TR25 to TR2

#### 4.2 The inverse problem

The inverse problem is to determine from the system response matrix (sensitivity matrices), a complex transformation matrix for converting the measured sensor values into pixel values. It is known as the tomogram. To reconstruct the tomogram requires an image reconstruction algorithm. The details for tomogram reconstruction are presented in the following section.

#### 4.3 Image reconstruction algorithm

To reconstruct the cross-section of an image plane from the projection data, the back-projection algorithm has been employed. Most of the work in process tomography has focused on the back-projection technique. It is originally developed for the X-ray tomography, and it also has the advantages of low computation cost (Garcia-Stewart et al., 2003). The measurements obtained at each projected data are the attenuated sensor values due to object space in the image plane. These sensor values are then back projected by multiply with the corresponding normalized sensitivity maps. The back projected data values are smeared back across the unknown density function (image), and overlapped to each other to increase the projection data density. The process of back-projection is shown in Figure 13, and Figure 14.

The density of each point in the reconstructed image is obtained by summing up the densities of all rays which pass through that point. This process may be described by Equation 4. Equation 4 is the back-projection algorithm where the spoke pattern represents blurring of the object in space.

$$f_b(x, y) = \sum_{j=1}^m g_j(x \cos \theta_j + y \sin \theta_j) \Delta \theta \quad (4)$$

where  $f_b(x, y)$  = the function of reconstructed image from the back-projection algorithm,  $\theta_j$  = the  $j$ -th projection angle, and  $\Delta\theta$  = the angular distance between projection, and the summation extends over all the  $m$ -projection.

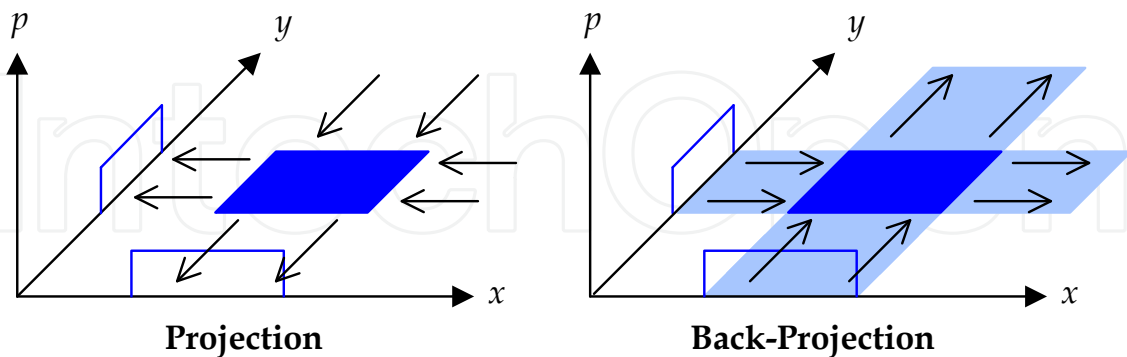


Fig. 13. The back-projection method

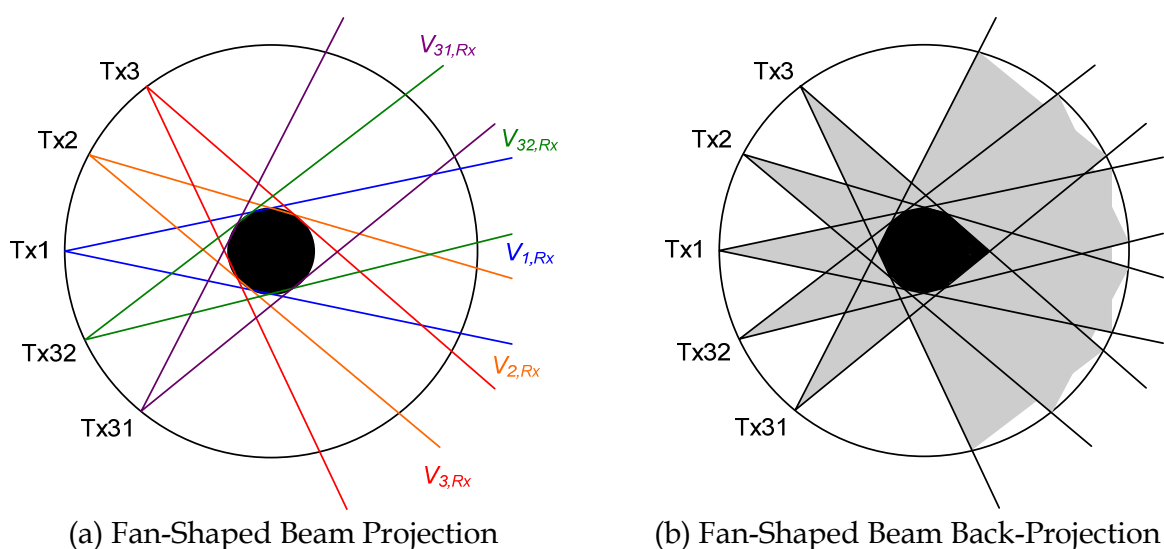


Fig. 14. The fan-shaped beam back-projection

#### 4.3.1 Linear back projection algorithm

The Linear Back Projection algorithm (LBP) is computationally straight forward to implement, and is a popular method for image reconstruction. Sensitivity maps, which were derived for the individual sensors are used by the LBP algorithm to calculate concentration profiles from measured sensor values. The process of obtaining concentration profile using LBP can be expressed mathematically as in Equation 5.

$$V_{LBP}(x, y) = \sum_{Tx=0}^m \sum_{Rx=0}^n S_{Tx, Rx} \times \overline{M}_{Tx, Rx}(x, y) \quad (5)$$

where  $V_{LBP}(x, y)$  is the voltage distribution on the concentration profile matrix,  $S_{Tx, Rx}$  is the sensor loss value, and  $\overline{M}_{Tx, Rx}(x, y)$  is the normalized sensitivity matrices.

#### 4.4 Image reconstruction results

The tomogram reconstruction on three phantoms of a small gas hold-up, a large gas hold-up, and a dual gas hold-up are shown in Figure 15, 16, and 17 respectively. The results showed several tomograms reconstructed using; (a) LBP, and (b) LBP with a threshold ratio of 0.55.

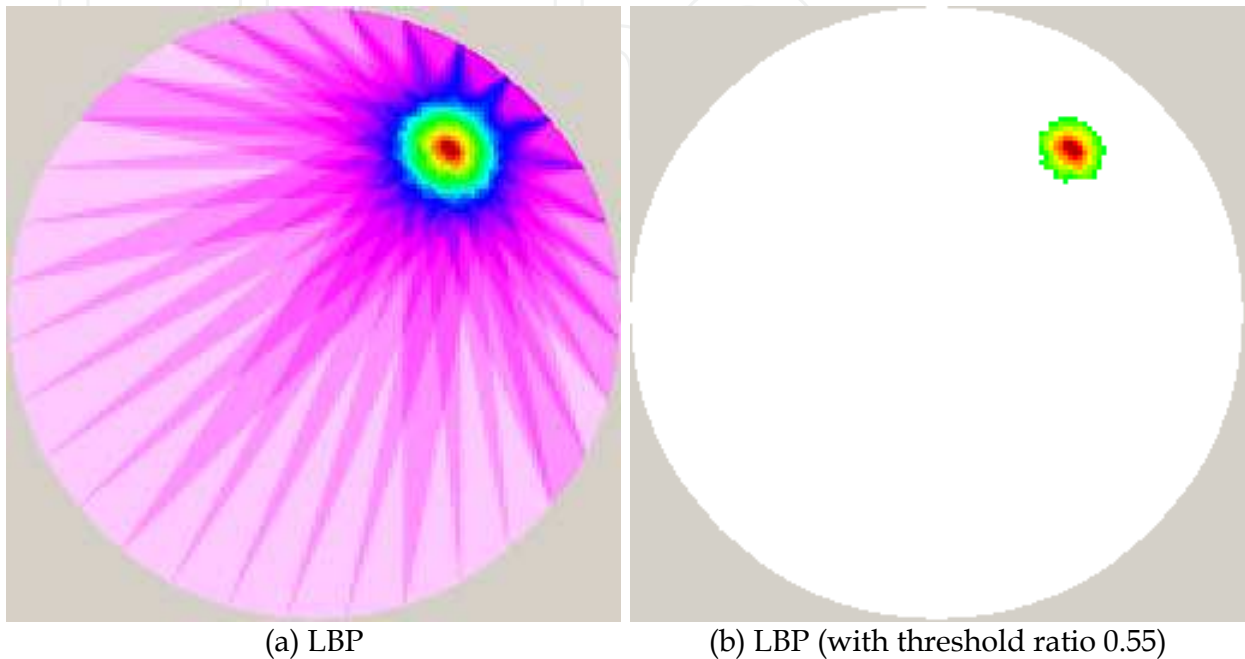


Fig. 15. Small gas hold-up

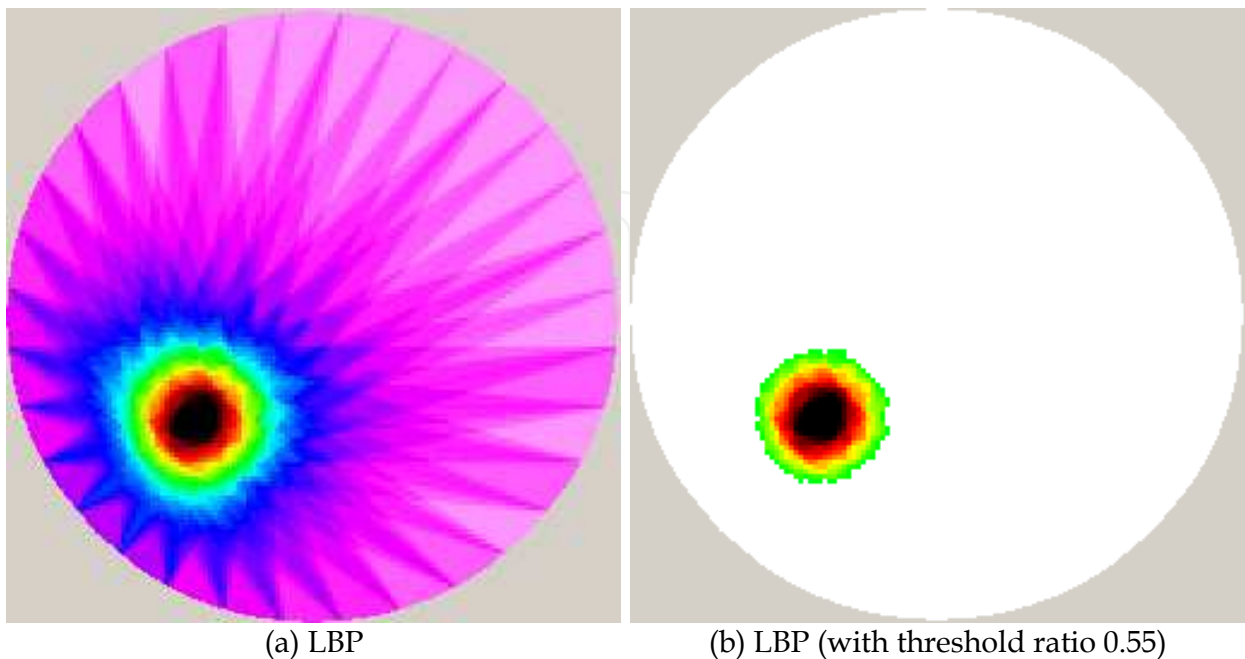


Fig. 16. Large gas hold-up

The tomogram in (a) showed that the LBP smears out, and introduces false images elsewhere. As seen in Figure 15(a), 16(a), and 17(a) the reconstructed images clearly contain qualitative information about the gas hold-up, but it is hard to distinguish the gas hold-up boundaries. However, the tomograms in Figure 15(a), 16(a), and 17(a) showed that the area of high gas concentration is clearly visible, and could be distinguished from the background image, and the shapes of the reconstructed images are reasonably accurate.

A thresholding technique has been used. To obtain the optimal threshold ratio, a further analysis has to be conducted by measuring the lowest error corresponds to the threshold ratio. By thresholding the image with a ratio of 0.55, the reconstructed images have tremendously improved. The smearing effects by back projection technique, which had caused non-uniformity of background image has been eliminated, and this is shown in Figure 15(b), 16(b), and 17(b). As a result, the information of liquid, and gas such as position, and shape could be easily obtained.

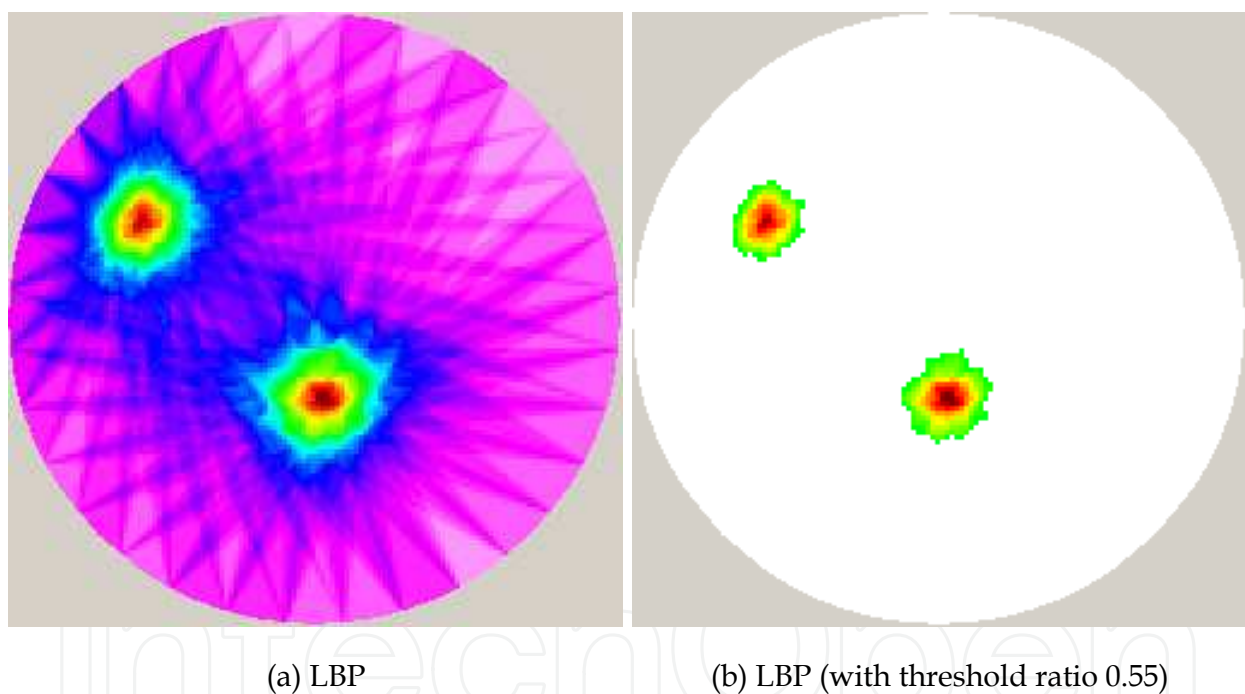


Fig. 17. Dual gas hold-up

## 5. Conclusions

The ultrasonic process tomography has been designed, and developed. The results show that the system could be used to identify, and locate the size, and position of gas bubbles in the measurement column. Experiments showed that, the image reconstructed by LBP results in blurring the image. This blurry image is due to the nature of back projection technique. However, the blurry image can be reduced by applying a thresholding technique. Hence, a clearly visible gas hold-up can be identified. This information is useful, and could be used for measuring the liquid/gas concentrations.

## 6. Acknowledgment

Authors are grateful to the financial support by Ministry of Higher Education Malaysia, Research University Grant from Universiti Teknologi Malaysia (Grant No. Q.J130000.7123.00J04), and Universiti Malaysia Perlis.

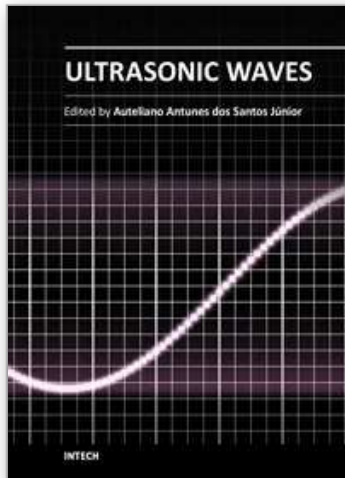
## 7. References

- Asher, R. C. (1983). Ultrasonic Sensors in the Chemical, and Process Industries. *Journal Science Instrument Physics*. Vol. 16, Pp. 959-963
- Broring, S., Fischer, J., Korte, T., Sollinger, S., & Lubbert, A. (1991). Flow Structure of The Dispersed Gas-phase in Real Multiphase Chemical Reactor- Investigated by A New Ultrasound-Doppler Technique. *Canadian Journal of Chemical Engineering*. Vol. 69, Pp. 1247-1256
- Garcia-Stewart, C. A., Polydorides, N., Ozanyan, K. B. & McCann, H. (2003). Image Reconstruction Algorithms for High-Speed Chemical Species Tomography. *Proceedings 3rd World Congress on Industrial Process Tomography*. Banff, Canada. 80-85
- Kannath, A. & Dewhurst, R. J. (2004). Real-Time Measurement of Acoustic Field Displacements Using Ultrasonic Interferometry. *Measurement Science Technology*. Vol. 15, Pp. 59-66
- Kytomaa, H. K. & Corrington, S. W. (1994). Ultrasonic Imaging Velocimetry of Transient Liquefaction of Cohesionless Particulated Media. *International Journal of Multiphase Flow*. Vol. 20, Pp. 915-926
- Moore, P. I., Brown, G. J. & Stimpson, B. P. (2000). Ultrasonic Transit-Time Flowmeters Modelled With Theoretical Velocity Profiles: Methodology. *Measurement Science Technology*. Vol. 11, Pp. 1802-1811
- Rahim, R. A., Rahiman, M. H. F., Zain, R. M., & Rahim, H. A. (2011). Image Fusion of Dual-Modal Tomography (Electrical Capacitance, and Optical) for Solid/Gas Flow. *International Journal of Innovative Computing, Information, and Control*. Vol. 7, No. 9, Pp. 5119- 5132
- Rahiman, M. H. F., Rahim, R. A., & Ayob, N. M. N. (2010). The Front-End Hardware Design Issue in Ultrasonic Tomography. *Sensors Journal*. Vol. 10, Issue 7, Pp. 1276-1281
- Rahiman, M. H. F., Rahim, R. A., & Zakaria, Z. (2008). Design, and Modelling of Ultrasonic Tomography for Two Component High Acoustic Impedance Mixture. *Sensors & Actuators: A. Physical*. Vol. 147, Issue 2, Pp. 409-414
- Rashidi, M. (1997). Fluorescence Imaging Techniques: Application to Measuring Flow, and Transport in Refractive Index-Matched Porous Media. *Chemical Engineering Technology*. Vol. 21, Pp. 7-18
- Sanderson, M.L. & Yeung, H. (2002). Guidelines for the Use of Ultrasonic Non-invasive Metering Technique. *Flow Measurement, and Instrumentation*. Vol. 13, Pp. 125-142
- Warsito, W., Ohkawa, M., Kawata, N., & Uchida, S. (1999). Cross-Sectional Distributions of Gas, and Solid Holdups in Slurry Bubble Column Investigated by Ultrasonic Computed Tomography. *Chemical Engineering Science*. Vol. 54, Pp. 4711-4728

Williams, R. A., & Beck, M. S. (1995). Process Tomography-Principles, Techniques, and Applications. Oxford, UK: Butterworth-Heinemann

IntechOpen

IntechOpen



## **Ultrasonic Waves**

Edited by Dr Santos

ISBN 978-953-51-0201-4

Hard cover, 282 pages

**Publisher** InTech

**Published online** 07, March, 2012

**Published in print edition** March, 2012

Ultrasonic waves are well-known for their broad range of applications. They can be employed in various fields of knowledge such as medicine, engineering, physics, biology, materials etc. A characteristic presented in all applications is the simplicity of the instrumentation involved, even knowing that the methods are mostly very complex, sometimes requiring analytical and numerical developments. This book presents a number of state-of-the-art applications of ultrasonic waves, developed by the main researchers in their scientific fields from all around the world. Phased array modelling, ultrasonic thrusters, positioning systems, tomography, projection, gas hydrate bearing sediments and Doppler Velocimetry are some of the topics discussed, which, together with materials characterization, mining, corrosion, and gas removal by ultrasonic techniques, form an exciting set of updated knowledge. Theoretical advances on ultrasonic waves analysis are presented in every chapter, especially in those about modelling the generation and propagation of waves, and the influence of Goldberg's number on approximation for finite amplitude acoustic waves. Readers will find this book a valuable source of information where authors describe their works in a clear way, basing them on relevant bibliographic references and actual challenges of their field of study.

### **How to reference**

In order to correctly reference this scholarly work, feel free to copy and paste the following:

Mohd Hafiz Fazalul Rahiman, Ruzairi Abdul Rahim, Herlina Abdul Rahim and Nor Muzakkir Nor Ayob (2012). Design and Development of Ultrasonic Process Tomography, *Ultrasonic Waves*, Dr Santos (Ed.), ISBN: 978-953-51-0201-4, InTech, Available from: <http://www.intechopen.com/books/ultrasonic-waves/design-and-development-of-ultrasonic-process-tomography>

**INTECH**  
open science | open minds

### **InTech Europe**

University Campus STeP Ri  
Slavka Krautzeka 83/A  
51000 Rijeka, Croatia  
Phone: +385 (51) 770 447  
Fax: +385 (51) 686 166  
[www.intechopen.com](http://www.intechopen.com)

### **InTech China**

Unit 405, Office Block, Hotel Equatorial Shanghai  
No.65, Yan An Road (West), Shanghai, 200040, China  
中国上海市延安西路65号上海国际贵都大饭店办公楼405单元  
Phone: +86-21-62489820  
Fax: +86-21-62489821

© 2012 The Author(s). Licensee IntechOpen. This is an open access article distributed under the terms of the [Creative Commons Attribution 3.0 License](#), which permits unrestricted use, distribution, and reproduction in any medium, provided the original work is properly cited.

IntechOpen

IntechOpen